Asian Journal of Chemistry; Vol. 35, No. 1 (2023), 45-51

ASIAN JOURNAL OF CHEMISTRY

https://doi.org/10.14233/ajchem.2023.24013

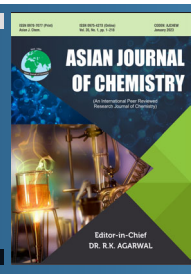

Hydrothermal Synthesis of Copper-Decorated Titanium Dioxide Spherulites and their Photocatalytic Activity against Reactive Dyes

G.K. SENDIL[1], E. SOUNDARRAJAN[1], M. ROSELIN RANJITHA[2], R.A. KLAIVANI[1,*] and S. RAGHU[3,*]

[1]Department of Chemistry, Vels Institute of Science, Technology & Advanced Studies (VISTAS), Chennai-600117, India
[2]Department of Chemistry, Stella Maris College (Autonomous) (Affiliated to University of Madras), Chennai-600086, India
[3]Centre for Advanced Research and Development (CARD)/Chemistry, Vels Institute of Science, Technology & Advanced Studies (VISTAS), Chennai-600117, India

*Corresponding authors: E-mail: subraghu_0612@yahoo.co.in; rakvani@yahoo.co.in

Received: 8 August 2022; *Accepted*: 9 October 2022; *Published online*: 27 December 2022; AJC-21076

The untreated discharge of industrial dyes into water supplies is a likely occurrence that can cause a number of dangerous scenarios that are hazardous for the ecology. Herein, a simple hydrothermal strategy for synthesizing copper-doped titanium dioxide nanoparticles (Cu-TiO_2) were presented and investigated its ability to photocatalytically degrade dyes *e.g.* reactive black 5 (RB5), red 198 (RR198) and yellow 145 dyes (RY145). Firstly, the as-synthesized Cu-TiO_2 nanoparticles were characterized using powder X-ray diffraction (PXRD), UV-diffuse reflectance spectroscopy (UV-DRS), high resolution-scanning electron microscopy (HR-SEM) and transmission electron microscopy (TEM) techniques. Furthermore, the photocatalysis experiments were conducted using three reactive dye solutions at different concentrations, pH, duration, *etc*. The spherulitic Cu-TiO_2 photocatalyst exhibited superior catalytic activity against the dyes and was able to achieve 82, 88 and 90% efficiencies for RB5, RR198 and RY145 dyes, respectively. The kinetics and the reusability parameters were also elaborated with respect to the obtained results. Therefore, Cu-TiO_2 spherulites are professed to be effectual photocatalyst materials for industrial scale dye degradation.

Keywords: Hydrothermal synthesis, Copper doped titanium dioxide, Spherulites, Photocatalysis, Reactive dyes.

INTRODUCTION

Devastation to the natural world has been an unintended consequence of emerging industrialization and technological breakthroughs over the past few decades. Specifically, the damage caused to essential resources of life such as water, air and soil leave behind harmful consequences to the entire ecosystem. Release of textile and industrial effluents into water reservoirs is a likely event that threatens the well-being of living creatures. Nearly 15% of dyes manufactured around the world unintentionally spread across and pollute the water systems [1]. This ultimately extends to a yearly count of 280,000 tons of dye being released in the form of effluents [2]. Such occurrences adversely impact the water's salinity, pH, total organic carbon, solid particle suspension, biological and chemical oxygen demand, *etc*. [3]. It is quantified that almost 70% of dyes that are manufactured for industrial scale usage are azo dyes that have large molecular weights and complex structural arrangement [4]. Azo dyes fall under the anionic variety of dye classification and is identified peculiarly with the presence of azo and sulphonic functional groups [5,6].

Dye effluent contaminated water dispel unpleasant odour over time, which results from the decomposition of hydrophytes and water-based entities. This occurs when the dye contamination escalates the water's turbidity and lowers the chance of receiving natural sunlight. In humans, ingestion of dye contaminated water leads to cancer, emphysema, heart diseases, dermatitis, kidney failure, metabolic stress, splenic sarcoma, *etc*. [7,8]. Owing to such risk factors and non-biodegradable nature, the quest for efficiently removing these harsh dye contaminants from the environment remains inevitable. Various strategies like photocatalysis, adsorption, ozonation, membrane filtration, enzyme degradation, reverse osmosis, electro-kinetic coagulation, *etc.* have been developed for the remediation of toxic dye moieties from industrial effluent discharge [9,10]. Amongst these approaches photocatalysis substantiates to be

the efficient, cost-effective and ecofriendly approach for remediation purposes. During this process reactive oxygen species like singlet oxygen, hydroxyl and superoxide radicals, *etc*. are generated which then attacks the toxic dye molecule and fragments it into safer products [11].

In recent times, the semiconducting materials are being used as photocatalysts owed to their diverse properties in various fields *e.g*. TiO_2, CuO, ZnO, Fe_2O_3, WO_3, Al_2O_3, SnO_2 and NiO are few of semiconductor metal oxides profoundly used for photocatalysis applications [12]. TiO_2 is widely studied as a photocatalyst owed to its eco-friendliness, cost effectiveness, stability and tunability. Doping it with certain elements is a proven way to tune its bandgap and harness its applicability in both ultraviolet and visible regions [13,14]. Liu *et al.* [15] synthesized xylan/PVA/TiO_2 composite and used it as a photocatalyst against astrazon brilliant red 4G and ethyl violet dyes. They successfully achieved about 94% degradation efficiencies for both the dyes. Simiarly, Mulpuri *et al.* [16] developed a TiO_2 co-doped with boron and zinc photocatalyst under sol-gel synthesis technique and successfully carried out the degradation of acid red 6 dye. D'Amato *et al.* [17] fabricated a gold/TiO_2 composite coated polypropylene matrix *via* dip coating method and investigated its ability to photodegrade alizarin red S dye. Chkirida *et al.* [18] synthesized a composite based on biopolymer sodium alginate, ferric/ferrous oxide and TiO_2 and tested its photocatalytic activity against methylene blue dye under ultraviolet light source.

In present work, nanoparticles of copper-doped titanium dioxide (Cu-TiO_2) were synthesized by hydrothermal synthesis and their use as a photocatalyst for the degradation of reactive black 5 (RB5), reactive red 198 (RR198) and reactive yellow 145 (RY145) dyes was demostrated. Dependence on the pH and concentration and pH of the dye solution, kinetics and recyclability were also be investigated.

EXPERIMENTAL

Titanium isopropoxide, copper acetate, trioctylphosphine oxide (TOPO), ethanol, reactive black 5 (RB5), reactive red 198 (RR198) and reactive yellow 145 (RY145) dyes were procured from Sigma-Aldrich, USA. Ultrapure distilled water was used throughout the study. PXRD pattern was obtained in a Rigaku SmartLab SE X-ray instrument at 20-80º diffraction angle. The UV-DRS patterns were recorded in a JASCO V-750 spectrophotometer at a wavelength sweep between 200-800 nm. The HR-SEM was done in a Thermoscientific Apreo S instrument whereas, HR-TEM images were taken in a JEOL JEM-2100 Plus instrument. The photocatalytic degradation studies were performed in a multi-lamp HEBER reactor aided with reflecting mirrors and six UV-Vis light sources.

Synthesis of Cu-TiO_2 nanoparticles: Copper acetate (0.05 M) and trioctylphosphine oxide (TOPO, 0.01 M) were added in a 1:4 ratio of ethanol:water solution under constant stirring. The resulting dispersion was added to 0.1 M titanium isopropoxide and stirred until a homogeneous mixture was obtained. Further, the mixture was transferred into a Teflon-lined autoclave setup which was placed in a hot air oven at 180 ºC for 10-12 h. The resultant hydrothermally synthesized Cu-TiO_2 was filtered out and washed several times with water and acetone to ensure purity. Then, it was vacuum sealed for further characterization and investigations.

RESULTS AND DISCUSSION

PXRD analysis: PXRD pattern (Fig. 1) was recorded for the Cu-TiO_2 nanoparticles to validate its formation and to find certain parameters like crystallite size, phases, purity, *etc*. The obtained spectrum accorded closely to the anatase-form of TiO_2 with standard JCPDS 21-1272 [19]. Dominant peaks at 25.3º, 37.8º, 47.9º, 54.3º and 62.72º were the characteristics of (101), (004), (200), (105) and (204) planes, respectively. These peaks and their corresponding planes exclude the probable formation of rutile or brookite forms of TiO_2 in the lattice. Thus, the phase purity of synthesized Cu-TiO_2 nanoparticles was validated accordingly. The crystallite size of Cu-TiO_2 nanoparticles was calculated to be 17 nm using the Debye Scherrer's equation. Additionally, it can be observed that the presence of copper dopant was not visibly detected in the spectrum. Yet, the existence of copper in crystal lattice is evident from the unusual broad peaks of the anatase-TiO_2. This broadness/wider appearance of the peaks can be attributed to the smaller grain sizes or the overlapping of rapid diffraction peaks [20]. However, owed to the incorporation of larger copper ions (ionic radii 0.72 Å) in comparison with the smaller titanium ions (ionic radii 0.68Å), copper ions tend to occupy the grain boundaries and thereby depresses further growth of the nanoparticle [21,22]. This leads to the unusual broader diffraction peaks of Cu-TiO_2 nanoparticles when compared to that of the standard anatase-TiO_2.

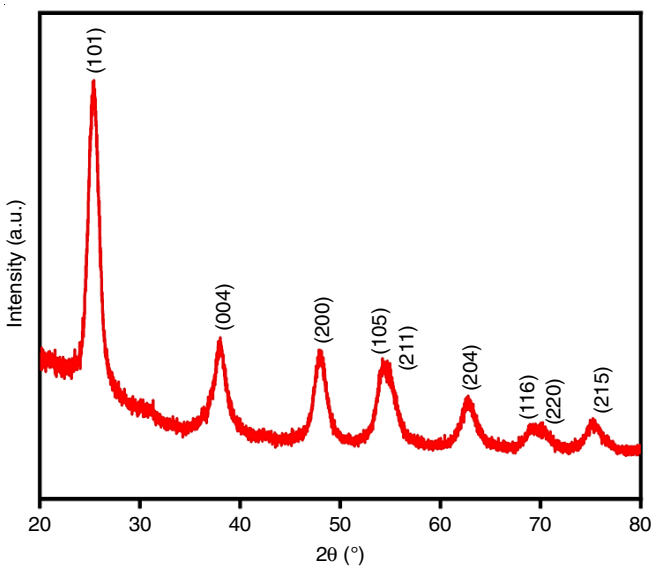

Fig. 1. PXRD pattern of Cu-TiO_2 nanoparticles

UV-DRS analysis: The optical absorbance and reflectance spectrum of Cu-TiO_2 nanoparticles were investigated and is displayed in Fig. 2a-b. A broad absorption maxima was centered at 300 nm and prolonged into the visible region of the spectrum. This is ascribed to the transport of charges between the valence and conduction bands, 2*p*-orbital of O^{2-} to the 3*d* t_{2g}-orbital of

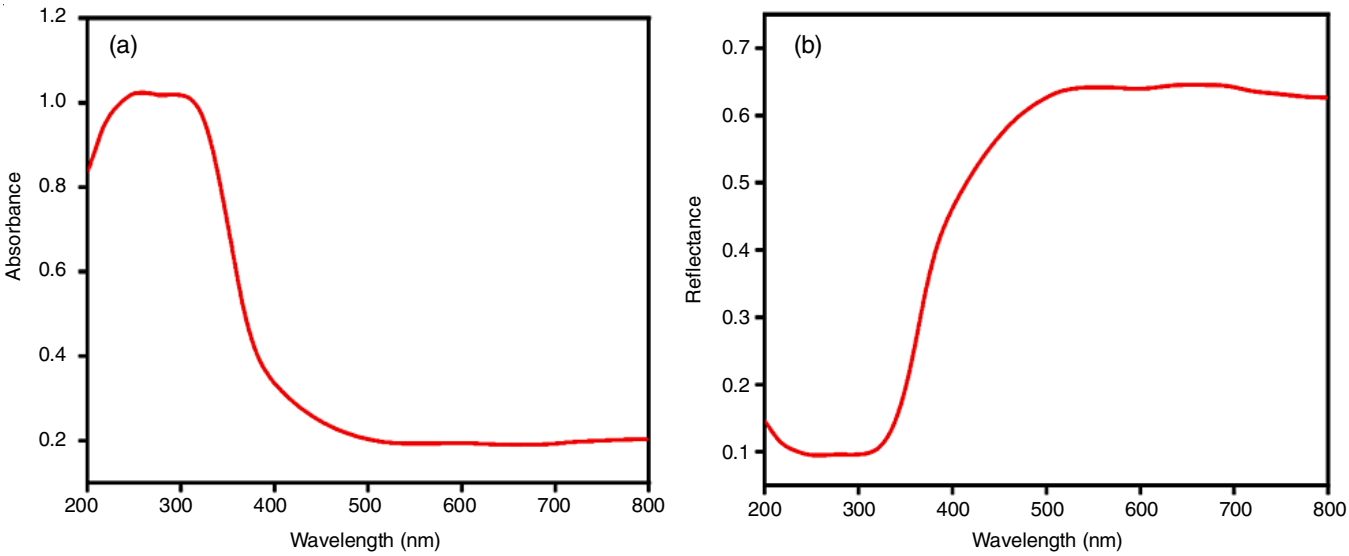

Fig. 2. (a) Absorbance and (b) reflectance spectrum of Cu-TiO_2 nanoparticles

Ti^{4+} [23]. The reflectance spectrum demonstrates that the nanoparticles can be employed in the visible range, as the diffused light can pass through at wavelengths greater than 400 nm. Fig. 3a-b exhibited the Kubelka-Munk plots [24], which were used to calculate the plausible bandgaps of the nanoparticles. The resulting bandgap energy (E_g) was found to be 3.3 and 3.2 eV for direct and indirect transitions, respectively. Such reduced bandgap values depict that the Cu-TiO_2 nanoparticles are capable of rapid electron transfer upon the incidence of a light source and therefore can act as an efficient photocatalyst.

Morphological studies: The morphological and particle size studies were briefly supported with HR-SEM and TEM analysis techniques. The HR-SEM image (Fig. 4a) showcased the formation spherulitic shaped Cu-TiO_2 nanoparticles. The particles were quite agglomerated due to the negligible attraction forces that act between the particles. The elemental composition was investigated with energy dispersive X-ray (EDX) study (Fig. 4b) and resulted in their corresponding atomic percentage values. The elements Ti, O and Cu were found to be present in 38.48, 58.59 and 2.92% compositions. This clearly puts forth the fact that copper has been successfully incorporated in the anatase-TiO_2 lattice. The average particle size of the spherulites were in the range of 350-450 nm. Also, the elements present in the sample were mapped and shown in Fig. 4c-e. Similar to the homogenous distribution of Ti and O elements, the Cu was also dispersed uniformly in the synthesized nanoparticles.

High resolution enhanced image of individual particles were obtained using HR-TEM analysis (Fig. 5a), which reconfirmed the spherulitic morphology of Cu-TiO_2 nanoparticles. Selected area electron diffraction fringes (SAED) (Fig. 5b) of Cu-TiO_2 nanoparticles were cross-referred with the JCPDS standard PXRD data and led to the major diffraction planes (101), (004) and (200). Similarly, the *d*-spacing value (Fig. 5c) were also calculated to be 0.358 and 0.194 nm, which corresponded to the characteristic diffraction planes (101) and (200) [25,26].

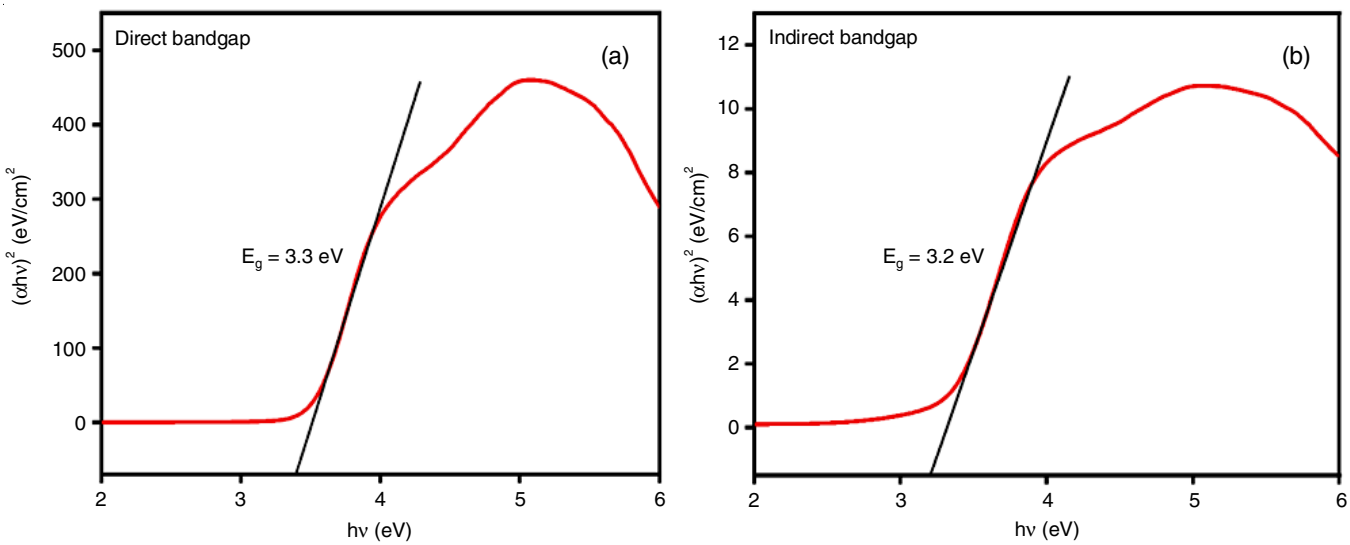

Fig. 3. Kubelka-Munk plots of (a) direct and (b) indirect bandgap plots of Cu-TiO_2 nanoparticles

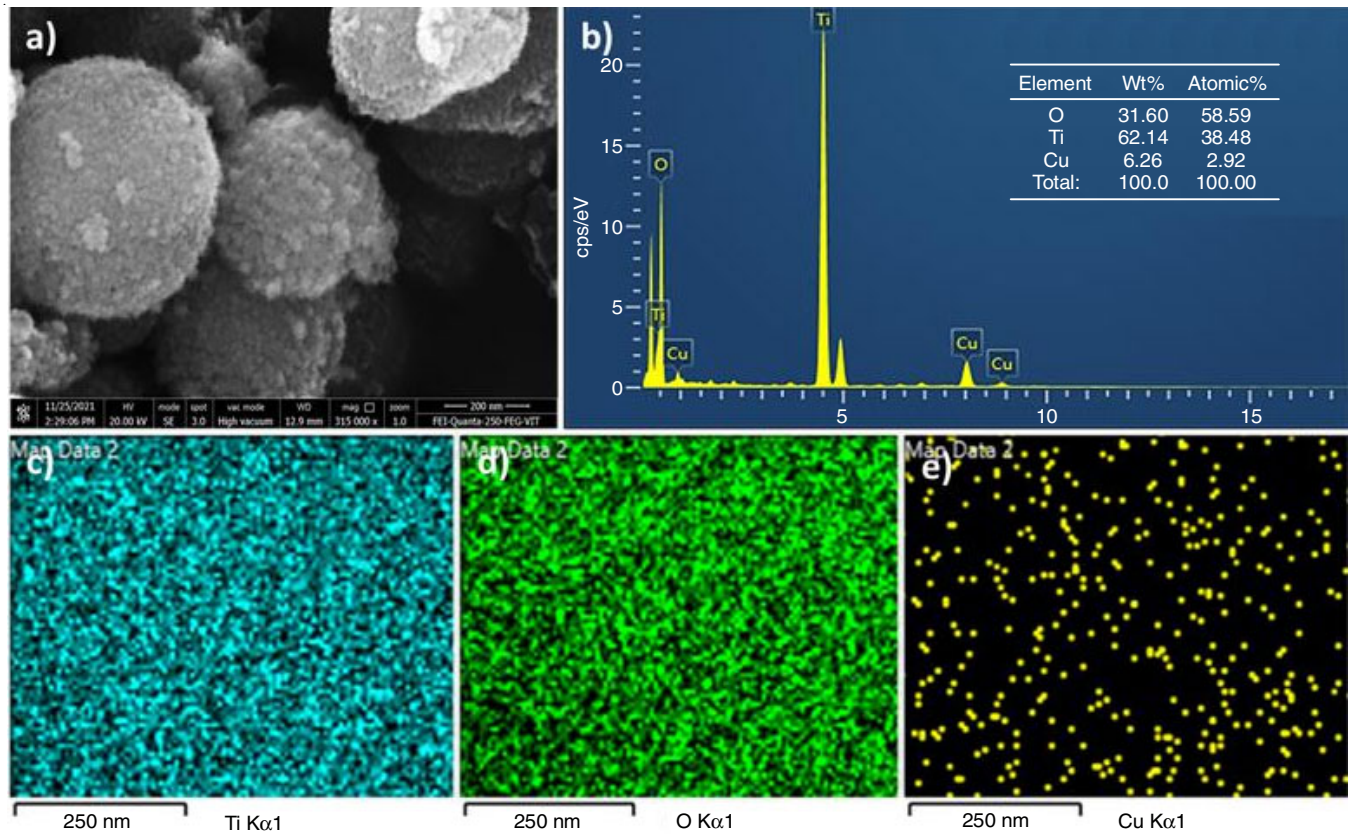

Fig. 4. HR-SEM (a) image, (b) EDX spectrum, inset-elemental compositions and (c-e) elemental mapping of Cu-TiO_2 nanoparticles

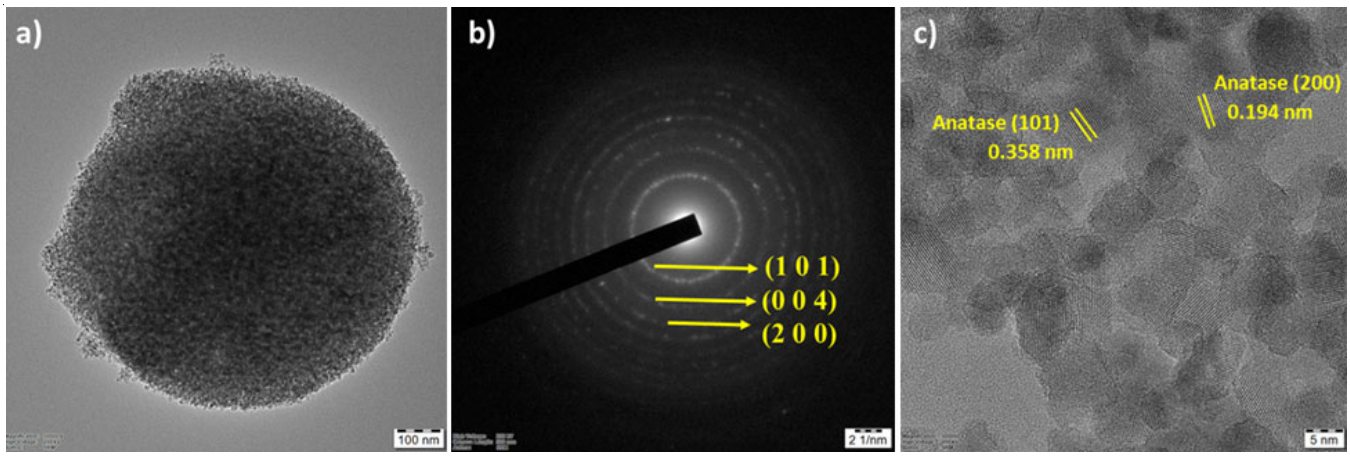

Fig. 5. HR-TEM (a) image, (b) SAED spectrum and (c) d-spacing of Cu-TiO_2 nanoparticles

Photocatalytic degradation of reactive dyes

Absorption studies: The 50 ppm solutions of RB5, RR198 and RY145 dyes were taken in 100 mL tubes made of quartz material and then 50 mg of Cu-TiO_2 photocatalyst was added in each tube before exposing the dye solutions to UV-Vis light. At a constant interval of 10 min, aliquots were retrieved and centrifuged to separate out the photocatalyst is dispersed in the solution from hindering the optical analysis. Further, the optical absorbance were recorded for the dye solutions and plotted against wavelength. As represented in Fig. 6, the absorbance intensity of all the three dye solutions were kept in contact with the photocatalyst reduced gradually under UV-Vis irradiation. The probable cause for the decreased absorbance is highly based on the photocatalytic activity of Cu-TiO_2 photocatalyst. When the surface of photocatalyst encounters UV-Vis light it excites and ejects a valence band electron of the photocatalyst to a high energy conduction band. Owed to this occurrence, a hole and an electron are left in the valence and conduction bands, respectively. These two entities initiate the formation of active species known as the reactive oxygen species (ROS). These ROS include hydroxyl radicals, which have the ability to degrade toxic dyes and transform them into gaseous carbon dioxide and water [27].

Effect of concentration and pH of dye solutions: The concentration dependence of the degradation was analyzed

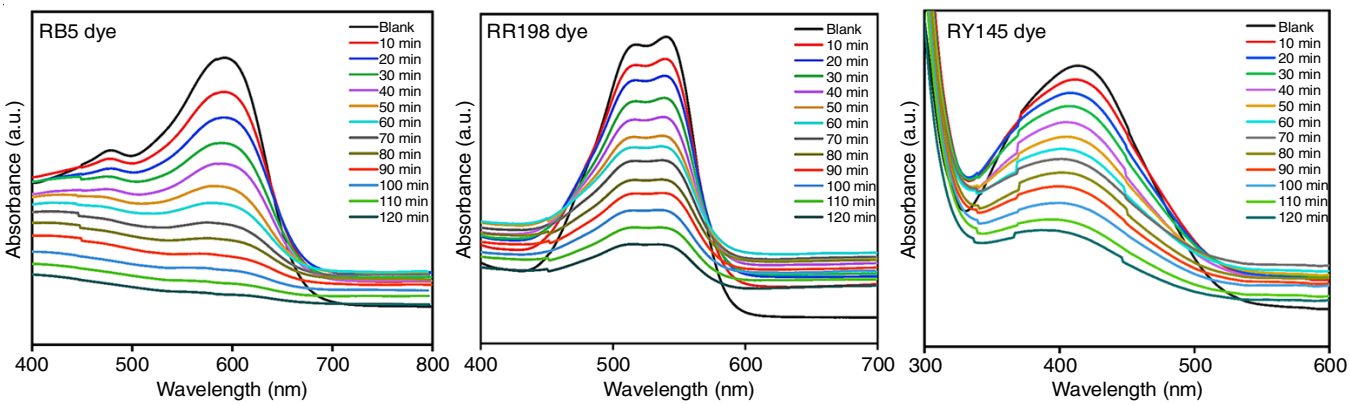

Fig. 6. Absorption spectra of 50 ppm RB5, RR198 and RY145 dye solutions in contact with Cu-TiO_2 photocatalyst

and is displayed in Fig. 7. An increased concentration is a direct illustration of the increased number of dye molecules in a solution. Every photocatalyst surface primarily requires a light source to activate the electron-hole recombination process which leads to photocatalytic degradation of dyes. However, when the dey concentration was increased beyond a certain extent the light source is obstructed by the increased presence of dye molecules. Such an act leads to lowered degradation and as a consequence the efficiency also declines [28]. In same way, when the concentration of the dye was increased from 25 ppm to 100 ppm, the efficiency declined drastically.

Similar to concentration, varying the pH of dye solution also impacts the degradation process. Since TiO_2 is a peculiar amphoteric material, it can adapt to varying pH conditions easily. Likewise, Cu-TiO_2 photocatalyst is also expected to have such equivalent characteristics. When the dye solution is adjusted to pH = 3, the photocatalyst surface acquires a positive charge and attracts the weakly negative charged dye molecules. The *vice-versa* happens when the solution pH is altered to 11. Fig. 8 showed that at both acidic and basis cases, the degradation efficiencies deviated from that of the degradation in neutral pH [29]. Collectively, the efficiencies were comparatively higher in acidic conditions and lower in basic condition with respect to neutral conditions.

Degradation efficiencies: Fig. 9 showed the maximum efficiency of degradation achieved by all the three studied dye solutions. The insets provide a visual evidence for the successful degradation of the dyes assisted by Cu-TiO_2 photocatalyst. The observed efficiencies were in the decreasing direction of RB5 > RR198 > RY145. The RB5 dye (89.31%) was degraded to a greater magnitude when compared to RR198 and RY145 dyes, which had efficiencies of 80.52 and 73.36%, respectively.

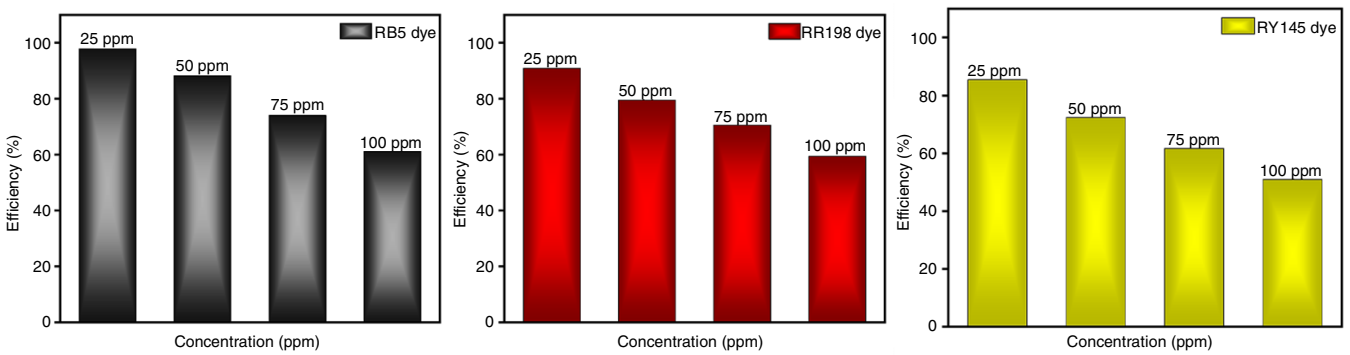

Fig. 7. Variation in degradation efficiency at different concentrations (25-100ppm) of RB5, RR198 and RY145 dye solutions

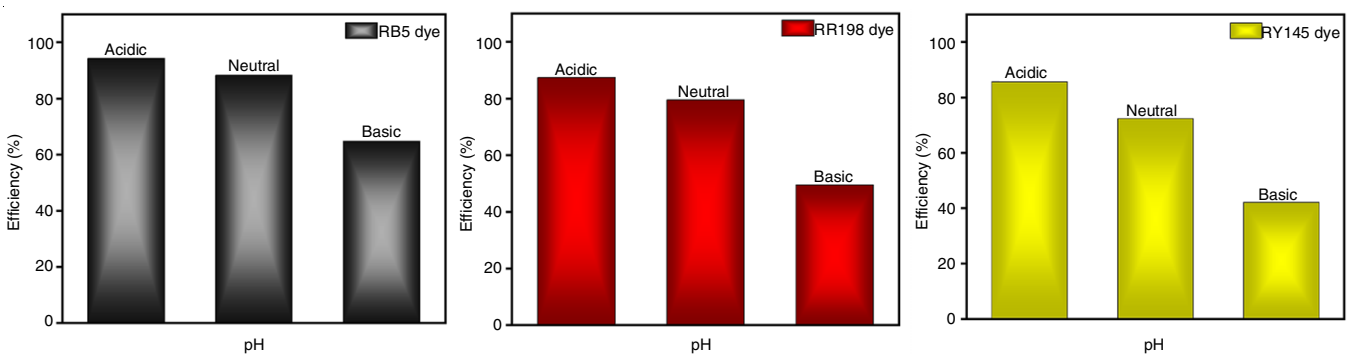

Fig. 8. Variation in degradation efficiency at different pH (3, 7 & 11) of 50 ppm RB5, RR198 and RY145 dye solutions

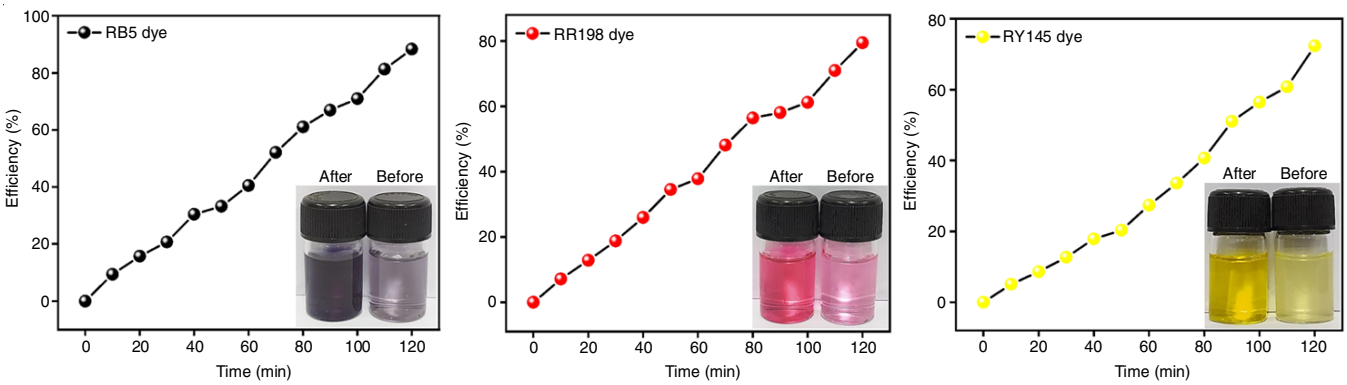

Fig. 9. Degradation efficiency of Cu-TiO_2 photocatalyst against 50 ppm of RB5, RR198 and RY145 dye solutions

It is clearly seen that the efficiency with respect to time didn't saturate completely in the stipulated 120 min duration. This infers that if the reaction progresses for further duration the Cu-TiO_2 photocatalyst can potentially degrade the dye moieties entirely.

Kinetic studies: The reaction kinetics of the degradation reaction was fit into the pseudo-1st order kinetic equation: $\ln (C_0/C) = k^1 t$ [30]. To find various parameters, the plot $\ln (C_0/C)$ against time was fitted into a linear graph (Fig. 10). Correlation coefficient (R^2), equilibrium time concentration (C_{eq} cal) and rate constant (k^1) were acquired from the linear fit and shown in Table-1. It was observed that the C_{eq} cal values were very low, which elucidates that the experimentally obtained dye concentrations would also be small. Hence, the Cu-TiO_2 photocatalyst's ability to degrade optimum concentration of the all three dyes is proven.

TABLE-1
PARAMETERS OF REACTION KINETICS

Dye	C_{eq} cal (mg g^{-1})	k^1 (min^{-1})	R^2
Reactive black 5	0.024	0.019	0.996
Reactive red 198	0.057	0.033	0.990
Reactive yellow 145	0.078	0.052	0.987

Recyclability/reusability study: Reusable nature of a photocatalyst material is a prominent feature that paves way for its commercial and industrial scale usage. This property of the prepared Cu-TiO_2 photocatalyst was verified by incorporating it into five continuous degradation cycles (Fig. 11). As a

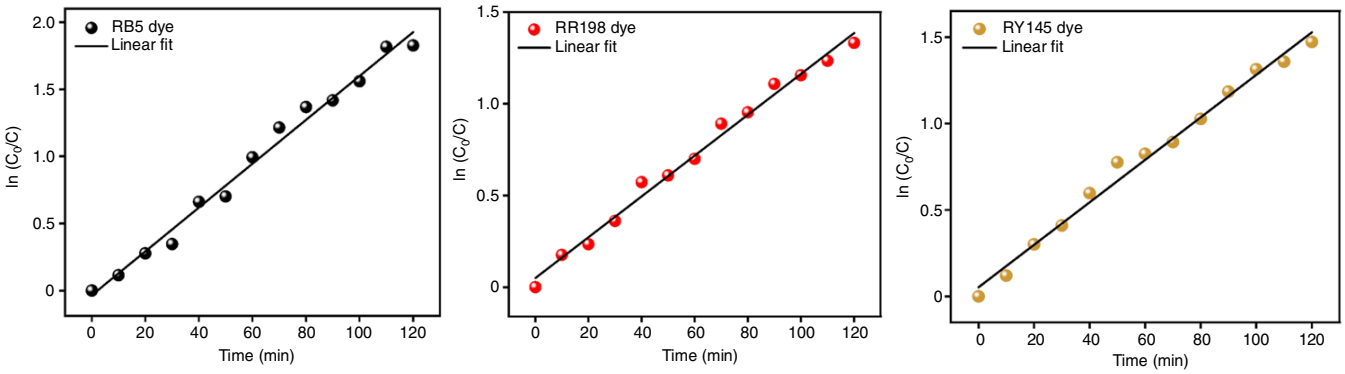

Fig. 10. Kinetics of photocatalytic degradation in 50 ppm of RB5, RR198 and RY145 dye solutions

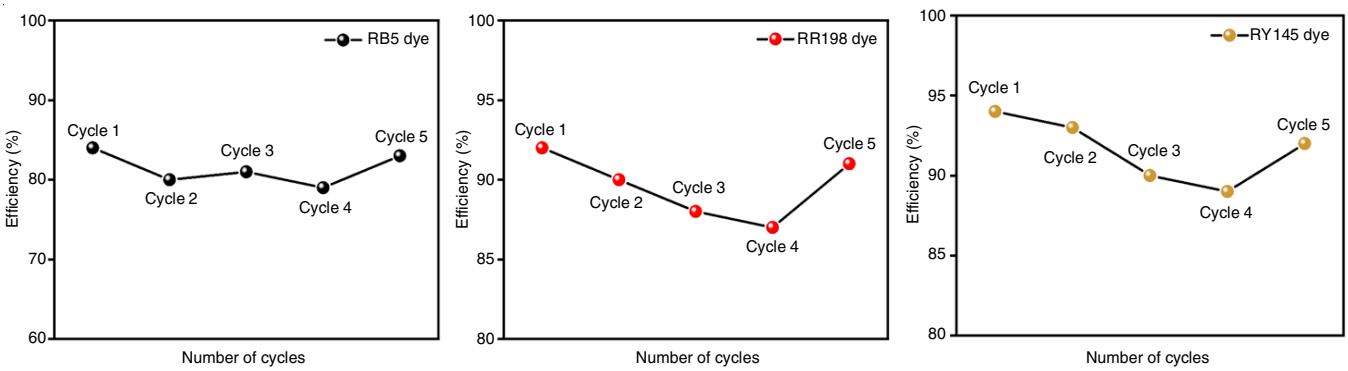

Fig. 11. Recyclability studies of Cu-TiO_2 photocatalyst in 50 ppm of RB5, RR198 and RY145 dye solutions

result the photocatalyst exhibited average efficiencies of 82%, 88% and 90% for RB5, RR198 and RY145 dyes, respectively. These values attested that the Cu-TiO_2 photocatalyst surface is highly active even after a number of degradation cycles and hence can be regenerated after multiple applications against harmful dyes.

Conclusion

The copper-doped titanium dioxide (Cu-TiO_2) spherulites were successfully synthesized *via* simple hydrothermal strategy. It was characterized and validated by PXRD, UV-DRS, HR-SEM and HR-TEM techniques. Further, it was incorporated as a photocatalyst for degrading three reactive dyes namely reactive black 5 (RB5), reactive red 198 (RR198) and reactive yellow 145 (RY145). Efficiency of the Cu-TiO_2 photocatalyst was studied at a wide range of dye concentrations 25-100 ppm. Studies of the dependence of degradation on pH were determined in acidic, basic, and neutral environments. Efficiency and kinetics of the degradation were also monitored with respect to time. Finally, the recyclability/reusability of Cu-TiO_2 photocatalyst was investigated under five continuous degradation cycles. Conclusively, this work endorses the Cu-TiO_2 nanoparticles as a superior photocatalyst material for real-time remediation applications.

CONFLICT OF INTEREST

The authors declare that there is no conflict of interests regarding the publication of this article.

REFERENCES

1. E.M. Saggioro, A.S. Oliveira, T. Pavesi, C.G. Maia, L.F.V. Ferreira and J.C. Moreira, *Molecules*, **16**, 10370 (2011); https://doi.org/10.3390/molecules161210370
2. M. Solís, A. Solís, H.I. Pérez, N. Manjarrez and M. Flores, *Process Biochem.*, **47**, 1723 (2012); https://doi.org/10.1016/j.procbio.2012.08.014
3. F. Mcyotto, Q. Wei, D.K. Macharia, M. Huang, C. Shen and C.W.K. Chow, *Chem. Eng. J.*, **2021**, 405 (2020); https://doi.org/10.1016/j.cej.2020.126674
4. S. Mishra and A. Maiti, *Environ. Sci. Pollut. Res. Int.*, **25**, 8286 (2018); https://doi.org/10.1007/s11356-018-1273-2
5. T. Shindhal, P. Rakholiya, S. Varjani, A. Pandey, H.H. Ngo, W. Guo, H.Y. Ng and M.J. Taherzadeh, *Bioengineered*, **12**, 70 (2021); https://doi.org/10.1080/21655979.2020.1863034
6. A. Sintakindi and B. Ankamwar, *Environ. Technol. Rev.*, **10**, 26 (2021); https://doi.org/10.1080/21622515.2020.1869322
7. P.K. Yeow, S.W. Wong and T. Hadibarata, *Biointerface Res. Appl. Chem.*, **11**, 8218 (2020); https://doi.org/10.33263/BRIAC111.82188232
8. R. Nithya, A. Thirunavukkarasu, A.B. Sathya and R. Sivashankar, *Environ. Chem. Lett.*, **19**, 1275 (2021); https://doi.org/10.1007/s10311-020-01149-9
9. O.T. Can, M. Kobya, E. Demirbas and M. Bayramoglu, *Chemosphere*, **62**, 181 (2006); https://doi.org/10.1016/j.chemosphere.2005.05.022
10. K. Sathishkumar, M.S. AlSalhi, E. Sanganyado, S. Devanesan, A. Arulprakash and A. Rajasekar, *J. Photochem. Photobiol. B*, **200**, 111655 (2019); https://doi.org/10.1016/j.jphotobiol.2019.111655
11. C.B. Li, F. Xiao, W. Xu, Y. Chu, Q. Wang, H. Jiang, K. Li and X.W. Gao, *Chemosphere*, **266**, 129209 (2021); https://doi.org/10.1016/j.chemosphere.2020.129209
12. S.P. Azerrad and E. Kurzbaum, *Water Air Soil Pollut.*, **232**, 40 (2021); https://doi.org/10.1007/s11270-021-04997-5
13. A. Yu, Q. Wang, J. Wang and C. Chang, *Catal. Commun.*, **90**, 75 (2017); https://doi.org/10.1016/j.catcom.2016.11.004
14. N. Riaz, F.K. Chong, Z.B. Man, R. Sarwar, U. Farooq, A. Khan and M.S. Khan, *RSC Adv.*, **6**, 55650 (2016); https://doi.org/10.1039/C6RA10371E
15. Z. Liu, R. Liu, Y. Yi, W. Han, F. Kong and S. Wang, *Carbohydr. Polym.*, **223**, 115081 (2019); https://doi.org/10.1016/j.carbpol.2019.115081
16. R.K. Mulpuri, S.R. Tirukkovalluri, M.R. Imandi, S.A. Alim and V.D.L. Kapuganti, *Sustain. Environ. Res.*, **29**, 1 (2019); https://doi.org/10.1186/s42834-019-0031-6
17. C.A. D'Amato, R. Giovannetti, M. Zannotti, E. Rommozzi, S. Ferraro, C. Seghetti, M. Minicucci, R. Gunnella and A. Di Cicco, *Appl. Surf. Sci.*, **441**, 575 (2018); https://doi.org/10.1016/j.apsusc.2018.01.290
18. S. Chkirida, N. Zari, R. Achour, A. Qaiss and R. Bouhfid, *Environ. Sci. Pollut. Res. Int.*, **28**, 14018 (2021); https://doi.org/10.1007/s11356-020-11664-5
19. X.J. Yang, S. Wang, H.M. Sun, X.B. Wang and J.S. Lian, *Trans. Nonferrous Met. Soc. China*, **25**, 504 (2015); https://doi.org/10.1016/S1003-6326(15)63631-7
20. Y. Zhang, Y. Meng, K. Zhu, H. Qiu, Y. Ju, Y. Gao, F. Du, B. Zou, G. Chen and Y. Wei, *ACS Appl. Mater. Interfaces*, **8**, 7957 (2016); https://doi.org/10.1021/acsami.5b10766
21. T. Aguilar, J. Navas, R. Alcántara, C. Fernández-Lorenzo, J.J. Gallardo, G. Blanco and J. Martín-Calleja, *Chem. Phys. Lett.*, **571**, 49 (2013); https://doi.org/10.1016/j.cplett.2013.04.007
22. N. Ghobadi, *Int. Nano Lett.*, **3**, 2 (2013); https://doi.org/10.1186/2228-5326-3-2
23. J.C.-T. Lin, K. Sopajaree, T. Jitjanesuwan and M.-C. Lu, *Sep. Purif. Technol.*, **191**, 233 (2018); https://doi.org/10.1016/j.seppur.2017.09.027
24. R.R. Mathiarasu, A. Manikandan, J.N. Baby, K. Panneerselvam, R. Subashchandrabose, M. George, Y. Slimani, M.A. Almessiere and A. Baykal, *Physica B*, **615**, 413068 (2021); https://doi.org/10.1016/j.physb.2021.413068
25. P. Pongwan, K. Wetchakun, S. Phanichphant and N. Wetchakun, *Res. Chem. Intermed.*, **42**, 2815 (2016); https://doi.org/10.1007/s11164-015-2179-y
26. A.A. Kashale, P.K. Dwivedi, B.R. Sathe, M.V. Shelke, J.Y. Chang and A.V. Ghule, *ACS Omega*, **3**, 13676 (2018); https://doi.org/10.1021/acsomega.8b01903
27. R. Rehman, Waheed-Uz-Zaman, A. Raza, W. Noor, A. Batool and H. Maryem, *J. Chem.*, **2021**, 6655070 (2021); https://doi.org/10.1155/2021/6655070
28. C. Tang and V. Chen, *Water Res.*, **38**, 2775 (2004); https://doi.org/10.1016/j.watres.2004.03.020
29. K.M. Reza, A. Kurny and F. Gulshan, *Appl. Water Sci.*, **7**, 1569 (2017); https://doi.org/10.1007/s13201-015-0367-y
30. R.R. Mathiarasu, A. Manikandan, K. Panneerselvam, M. George, K.K. Raja, M.A. Almessiere, Y. Slimani, A. Baykal, A.M. Asiri, T. Kamal and A. Khan, *J. Mater. Res. Technol.*, **15**, 5936 (2021); https://doi.org/10.1016/j.jmrt.2021.11.047